Novel Reconfigurable Intelligent EBG Metasurface Layer for ASK Modulation

Hayder Almizan
University of Kufa
Taha A. Elwi (taelwi82@gmail.com)
Al-Mammon University College https://orcid.org/0000-0002-8389-5457
Zaid A. Abdul Hassain
Mustansiriyah University

Research Article

Keywords: ASK Modulator, reconfigurable EBG layer, microstrip antenna, gain enhancement, Direct Antenna Modulation (DAM).

Posted Date: March 16th, 2021

DOI: https://doi.org/10.21203/rs.3.rs-260100/v1

Novel Reconfigurable Intelligent EBG Metasurface Layer for ASK Modulation

Hayder Almizan[1], Taha A. Elwi[2], Zaid A. Abdul Hassain[3]
[1]Department of Electronics and Communications, College of Engineering, kufa University, Najaf, Iraq
[2]Communication Engineering Department, Al-Ma'moon University College, Baghdad, Iraq
[3]Electrical Engineering, College of Engineering, Mustansiriyah University, Baghdad, Iraq
Corresponding author: Taha A. Elwi (taelwi82@gmail.com) and (tahaelwi82@almamonuc.edu.iq).

ABSTRACT In this paper, a novel structure of a reconfigurable Electromagnetic Band Gap (EBG) layer is presented for direct antenna Amplitude Shift Keying (ASK) digital modulation. Therefore, the modulation process, in this paper, is realized without the need to include conventional parts like filters, mixers or power amplifiers. Beside many advantages, the proposed modulation process offers cost, complexity, and weight reductions to suit many modern applications including 5G systems. The reconfigurable EBG layer has two statuses: ON and OFF. Each status produces a certain level of gain enhancement. Via controlling the reconfigurable EBG statuses, the amplitude of the transmitted wave can be controlled. The results show such a system design can modulate the electromagnetic signals directly by varying the gain from 2 dBi for logic_0 (OFF) to 11 dBi for logic_1 (ON). For this, a mathematical model based on ray tracing analysis is conducted to explain the principle of operation of the proposed EBG layer. The antenna and EBG structures fabrication as a system is realized and tested experimentally. The measurements show good agreements with the proposed mathematical model and CST MWS simulations.

INDEX TERMS: ASK Modulator, reconfigurable EBG layer, microstrip antenna, gain enhancement, Direct Antenna Modulation (DAM).

I. INTRODUCTION

ASK is one of the digital modulation techniques for wireless communication where the carrier amplitude is adjusted according to the baseband data values [1]. The data is mapped to a carrier wave with low power, and then the carrier wave is amplified and filtered to provide a suitable wave for transmission over a channel through a passive transmitting antenna. Filters, mixers, and power amplifiers represent the main parts of any conventional ASK modulation [2]. Eventually, disadvantages like complexity, non-linear effects of the power amplifier and high cost, among others, are inevitable in such modulation systems [2].

Direct Antenna Modulation (DAM) has emerged as a practical solution to overcome some of these disadvantages. The basic idea behind DAM is to allow modulation of the carrier wave at the antenna structure [2]. Reconfigurable antenna system designs may satisfy the need for smart microwave systems; however, they still very limited for most types of modulation. Various approaches of DAM have been presented, based on array of switchable passive reflectors [3]. Pulse duration modulation was achieved directly with a MIMO system through the time switching for the antenna elements [4]. A constellation in the far-field was produced by varying the antenna load and current [5].

On the other hand, many researchers realized the use of EBG layers to enhance the antenna performance. For example, a design based on an EBG layer was introduced to enhance the antenna gain; however, the design does not consider the reconfiguration approach [6]. High gain antenna based on three layers was proposed to enhance the gain at certain level without including smart applications [7]. In [8], authors introduced an approach to explore the design of high gain antenna with a wide band by introducing a Gaussian lens. Fabry Perot cavity was introduced to enhance the antenna gain at millimeter waves [9]. A near-field direct antenna modulation was introduced in [10] to achieve time modulation communication link. A design of a high gain antenna based on EBG layer was presented in [11] and developed furthermore in [12] to realize gain variation through changing the EBG array dimensions. In [13] and [14], the authors discussed the physics and analysis of the metasurface operation for gain enhancements based on Furrier optics and ray tracing analysis, respectively.

Later, another approaches presented recently based on smart coded metasurface including EBG layers as reflectors [15]-[20]. For instance, the proposed metasurface in [15] was designed to realize an 8-phase shift keying wireless transmitter. In [16], an ASK modulation technique was proposed based on switchable metasurface at THz applications. A phase shift keying was developed based a smart metasurface in [17] using varactor diodes to change the phase level of the antenna. A reprogrammable hologram was produced based a one bit metasurface for imaging applications [18]. A microwave imaging was proposed based on 2-bit programmable metasurface for single sensor and single frequency in [19]. A scattering diffusion was improved in [20] using an active metasurface at THz frequencies. However, all the previous listed research papers used reflector arrays as metasurfaces that are very limited to the antenna type. Therefore, their use for planer antennas including microstrip structure is not applicable.

Later, the use of transmitarray metasurfaces, EBG layer, was introduced to show no limitations with the antenna type [21]. Moreover, different advantages in the programmable metasurfaces attracted researches; because their excellent capabilities in controlling the antenna beam forming in terms of amplitude, main lobe direction, and beam width [22]; in which the electromagnetic wave modulation can be

obtained by varying the coefficients (transmission or reflection) distribution electrically on the metasurfaces [23]. For this, the authors of this paper are motivated on combining a novel programmable EBG layer with a traditional circular polarized microstrip antenna to realize gain enhancement for ASK modulation. Therefore, two statues are synthesized, logic_1 or logic_0, to achieve a programmable metasurface.

In this paper, a design of an ASK modulator based on a reconfigurable EBG layer is presented. The proposed ASK modulator promises to solve the non-linearity problem of the power amplifier as well as reduces the transmitter complexity and cost. Nevertheless, most previous published papers conducted their work based on reflector array and high gain horn antenna, however, this research realizes the use of EBG layer to reconfigure the antenna gain for ASK modulation. Thus, the advancements of using the EBG layer over reflect arrays that can be summarized through size reduction, no limitation at antenna type, less complexity, and more robust [12]; motivated us to use derived EBG unit cell from Journalism cross geometry.

II. RECONFIGURABLE EBG LAYER AND ANTENNA STRUCTURES

The proposed EBG layer is based on an array of 5×5 unit cells. To realize the configuration purpose, the individual unit cell is constructed from striplines and crosses that controls the current motion using active devices; which unlike to the limitations of traditional apertures and/or patches [11]. Therefore, the individual unit cell is based, basically, on a Jerusalem cross section with four L-shape strips to perform current motion control. However, the purpose of adding the L-shape strips is to enhance the equivalent LC circuit to obtain the desirable S-parameters at the frequency band of interest. Four pin diodes are inserted to have the reconfiguration mechanism for gain control behavior; therefore, the striplines width is selected to suit the pin diodes dimensions. In Fig. 1, the proposed unit cell is presented where the proposed unit cell dimensions are listed in Table I and adjusted to resonant at 2.7 GHz.

The maximum unit cell dimension is utilized at 60 mm to suit the EBG design criterion [23]; at which the unit cell size is related to λ/2. Therefore, breaking the unit cell at the center by adding a PIN diode may realize a different unit cell configuration with different characteristics. Nevertheless, four diodes sharing the same ground are used instead of one diode to realize a gain control along the azimuth and zenith at the same time. Thus, a symmetric radiation pattern would be achieved from such configuration.

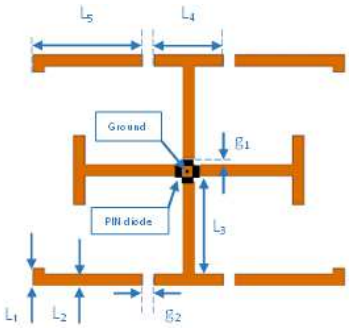

FIGURE 1. EBG unit cell structure.

TABLE I. EBG unit cell dimensions.

parameter	*dimension in (mm)*
L_1	*3*
L_2	*2*
L_3	*17*
L_4	*12*
L_5	*19*
g_1	*1*
g_2	*2*

Now the EBG layer that is constructed from the proposed unit cell is mounted on a flexible thin layer of, 0.1 mm thickness, FR4 substrate. The overall individual unit cell dimensions are 60 mm x 60 mm where the physical dimensions of the unit cell are 54 mm x 40 mm as well as spaces between neighbored unit cells are 3 mm on x-axis and 10 mm on y-axis. To ensure minimum coupling between unit cells, the periodicity of unit cell is adjusted to be 60 mm (~λ/2) [12].

In general, the effective unit cell dimensions are asymmetrical; the length is not equal to the width, the reason of that is to obtain symmetrical output radiation patterns through astigmatism phenomena [14]. Moreover, the purpose of having 5×5 array is to reduce the total internal reflection that causes sever back radiations, also, minimizing the diffraction losses due to the electromagnetic fringing from the layer edges [13]. Therefore, the proposed EBG layer area is 294 mm × 294 mm as seen in Fig. 2.

The resulted EBG layer, see Fig. 2(a), is located at 70 mm from the top of a patch microstrip antenna that is presented in Fig. 2(b). The reason of considering such distance is to locate the antenna at the focal point from the EBG layer within the limitation of the numerical lens aperture [16]. Fig. 2(b) shows the design of the proposed microstrip antenna. The patch geometry is inspired from [12] based on truncated rectangular structure to provide circular polarization 2.45 GHz. Nevertheless, the slots insets are etched from the patch to enhance the matching impedance below -10 dBi. Therefore, with a single feed the circular polarized can be achieved, however, the radiation pattern symmetry could be ruined [14]. The substrate dimensions are 294 mm × 294 mm of FR4 material with ϵ_r= 4.4 and thickness of 2 mm. The ground plane is mounted on the other side of the substrate. The patch dimensions are listed in Table II.

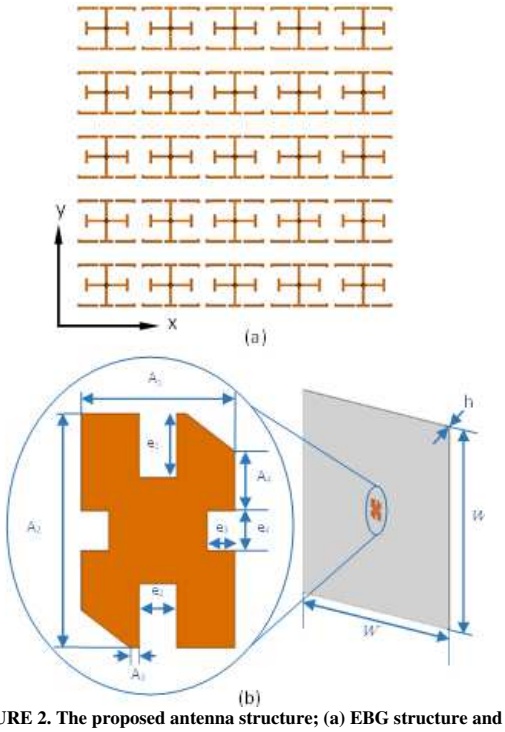

FIGURE 2. The proposed antenna structure; (a) EBG structure and (b) Microstrip antenna.

TABLE II. The proposed reconfigurable EBG unit cell dimensions.

parameter	*Dimension (mm)*
W	*294*
h	*2*
A_1	*19.31*
A_2	*27.43*
A_3	*1.17*
A_4	*6.98*
e_1	*7.51*
e_2	*4.66*
e_3	*3.44*
e_4	*4.65*

III. THEORY OF EBG-ANTENNA OPERATION

The concept of the focal length is an essential point must be considered for both unit cell statuses: in case of ON and/or OFF. The reason for such interest is due to the maximum gain can be achieved when the distance between the EBG layer and the antenna is relative to the focal length, tuned, to obtain the paraxial rays [14]. Consequentially, each unit cell shows two different values of the focal length one for logic_1 and the other for logic_0.

The present work with the proposed EBG layer at logic_1 is formed to reach the maximum gain enhancement when it is located at the focal point. In case of switching the EBG layer to logic_0, the focal length would be changed to another value at minimum gain enhancement, while, the distance between the EBG layer and the antenna remains constant; this means a reduction in the antenna gain level could be achieved. Such procedure introduces two distinguished levels of gain controlled via the status of the EBG layer to define ASK as seen in Fig. 3.

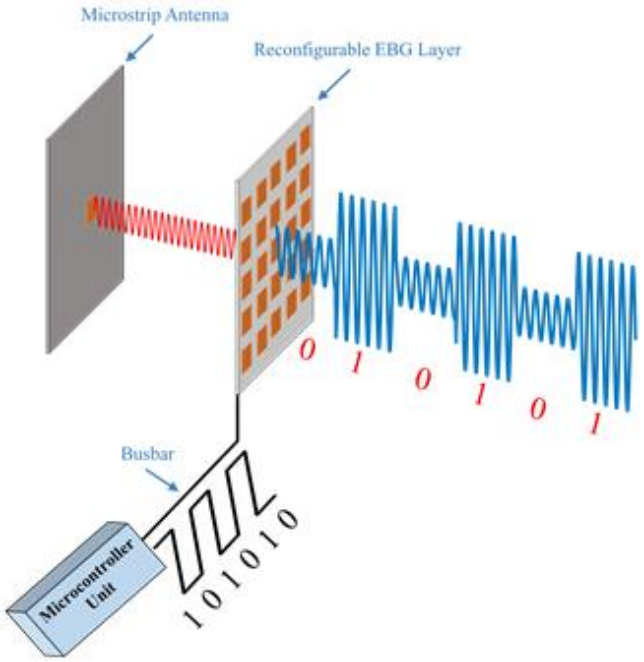

FIGURE 3. System schematic of the proposed ASK modulator.

Based on ray tracing analysis that is inspired from the optical theory [13], authors explored the principle operation of the EBG layer as a lens mountain antenna and make the necessary calculations. The synthesis of the proposed EBG layer follows two considerations: Firstly, the proposed EBG layer has dimensions equals or less than the dimensions of the microstrip antenna ground plane. This consideration is to reduce as much as the side lobes levels. Second, the phase difference between any two neighboring unit cells on the EBG layer diagonal is designed to be $\sqrt{2}\,\pi$ rad for an incident electromagnetic wave. As shown in Fig. 4, the phase difference is given by [8]:

$$k[R_i - (\vec{r}_i.\hat{r}_\circ)] = \psi_i - \psi_\circ \qquad (1)$$

where k is the propagation constant of the free space, the distance from the patch antenna center to the i^{th} element center is represented by R_i, $\vec{r}_i$ is the position vector of i^{th} element, while the direction vector of the main beam is $\hat{r}_\circ$.

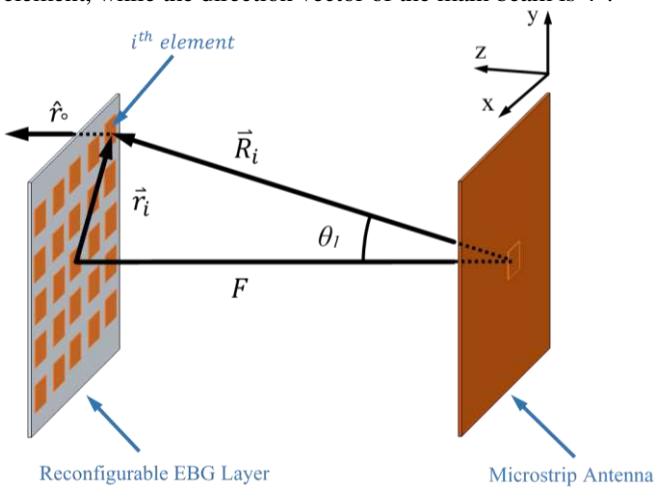

FIGURE 4. Ray tracing based phase difference.

The term $\psi_i - \psi_\circ$ represents the phase difference between the normal incident ray and extreme emerging ray. At the broadside direction, the phase difference is doubled to equal $2\sqrt{2}\,\pi$ rad. The other clue at the broadside direction is that both $\vec{r}_i$ and $\hat{r}_\circ$ are almost perpendicular, which mean θ_2 is a very small value. Assuming θ_2 has value of 2°, the result of $\vec{r}_i$ and $\hat{r}_\circ$ dot product is $120\sqrt{2}\ cos(90° - \theta_2)$. According for pervious boundaries, the value of R_i is 183.5 mm and θ_1=67.6°. On the other hand, the antenna gain is inversely proportional to both θ and φ angles [9].

$$G \propto \frac{1}{\theta\varphi} \tag{2}$$

where θ is the elevation angle at the E-plane and φ is the azimuth angle at the H-plane in degrees. For symmetry in the radiation pattern we assumed θ=φ. Therefore, reducing θ and/or φ realizes a significant increase in the antenna gain. Such that, a significant change could be reflected on the focal length of the EBG layer as seen in the derived equation:

$$F = \frac{\left(\frac{D}{2}\right)}{tan\,\theta_1} \tag{3}$$

where D is the diagonal of the EBG layer and it could be to twice of $|\vec{r}_i|$ or $\sqrt{2}\,W$. θ_1 is the angle of incident wave on the EBG layer and equals to half of θ approximately. The resulted focal distance would be 70 mm. Fig. 5 shows the change of the focal distance F with respect to θ_1. Therefore, it is clearly, increasing the angle of the incident wave results to decrease the focal distance.

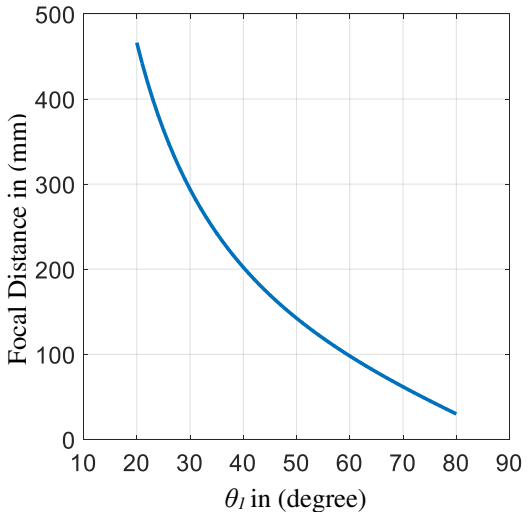

FIGURE 5. Ray tracing analysis.

Fig. 6 shows the applied ray tracing process. The antenna is assumed the source of the electromagnetic field. It is assumed that the electromagnetic rays are diverging away from the patch surface as shown in Fig. 6(a). The extreme rays are incident to the back side of the EBG layer with angle of θ_1 as depicted in Fig. 6(b) and refracted away from the top surface of the EBG layer with an angle of θ_2. Applying the ray tracing on the extreme rays as shown in Fig. 6(c), the focal length could be significantly affected with θ_1 according to Snell's law. The equation of the refraction angle θ_2 [14] is given by:

$$\theta_2 = sin^{-1}\left[\left(\frac{n_1}{n_2}\right) sin\,\theta_1\right] \tag{4}$$

where n_1 is the free space refractive index which is one and n_2 is the EBG layer refractive index that is relative to the unit cell. However, Fig. 6(d) shows the other rays path when they are reflected away for the back side of the EBG layer due to the total internal reflection phenomena that will be studied later on.

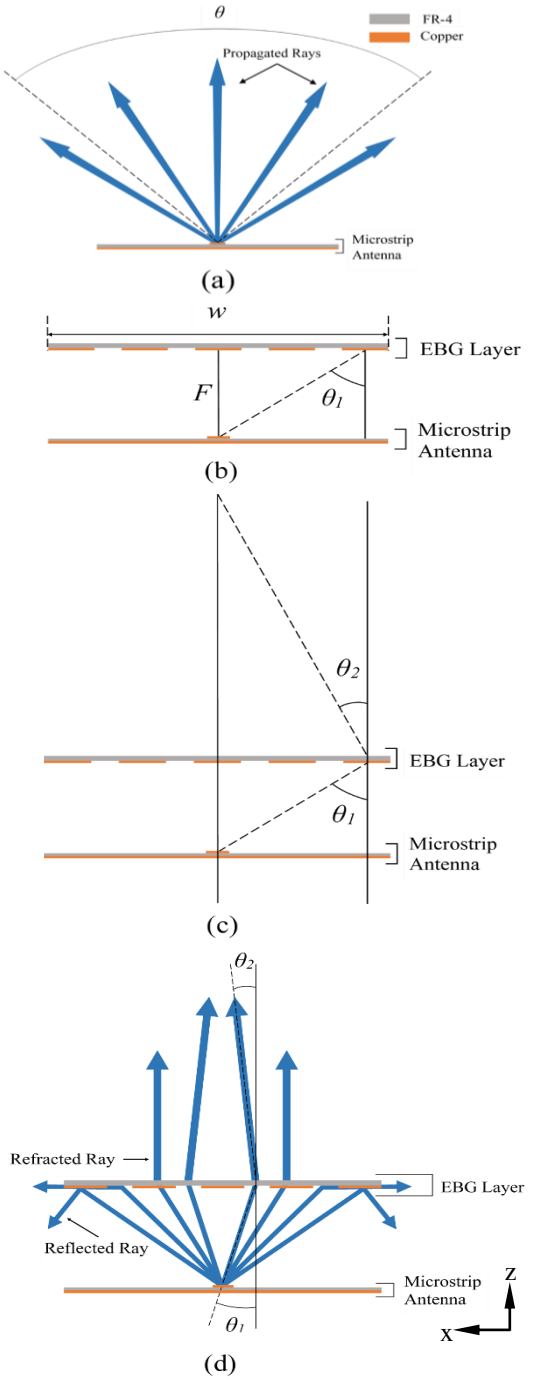

FIGURE 6. Ray tracing analysis; (a) diverging beams from the antenna, (b) extreme beams incidence, (c) beam refraction, and (d) total internal reflection.

Now, the curve in Fig. 7 displays the effects of varying (n_2) with respect to the refraction angle θ_2. The noticed point in Fig. 7 is that when n_2 approaches minus infinite, θ_2 goes to be zero which means the resulting beam is paraxial. Consequently, gain enhancement would be dependent on the value of n_2. The proposed EBG unit cell dimensions are changing by switching the unit cell ON and/or OFF. This property leads to change n_2 value to realize a change in the antenna gain enhancement through varying the focal length as discussed previously.

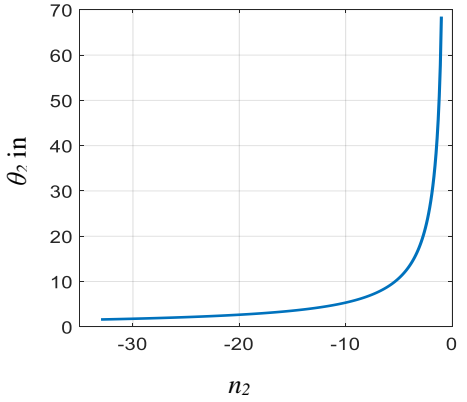

FIGURE 7. Changing of θ_2 with respect to n_2 according to Snell's law.

In another aspect, the EBG focal length can be related to θ_1 with respect to the value of n_2 as given by equation (5):

$$F = \frac{\left(\frac{D}{2}\right)}{tan\left(sin^{-1}\left[\left(\frac{n_2}{n_1}\right)sin\,\theta_2\right]\right)} \qquad (5)$$

The angle θ_2 is 2° as assumed previously, and n_2 is a value more than -1. The focal distance increases when n_2 decreases as seen in Fig. 8. The reconfigurable EBG layer, at perpendicular and parallel polarizations can be followed as:

$$\Gamma_{/\!/} = \frac{n_1 cos\theta_2 - n_2 cos\theta_1}{n_1 cos\theta_2 + n_2 cos\theta_1} \qquad (6.A)$$

$$\Gamma_{\perp} = \frac{n_1 cos\theta_1 - n_2 cos\theta_2}{n_1 cos\theta_1 + n_2 cos\theta_2} \qquad (6.B)$$

where, $\Gamma_{/\!/}$ and $\Gamma_{\perp}$ are the reflection coefficients at parallel and perpendicular polarizations, respectively, are presented in Figs. 8(b) and 8(c). Thus, there is TIR for incident rays from the rare to denser medium, irrespective of whether the polarization is perpendicular or parallel.

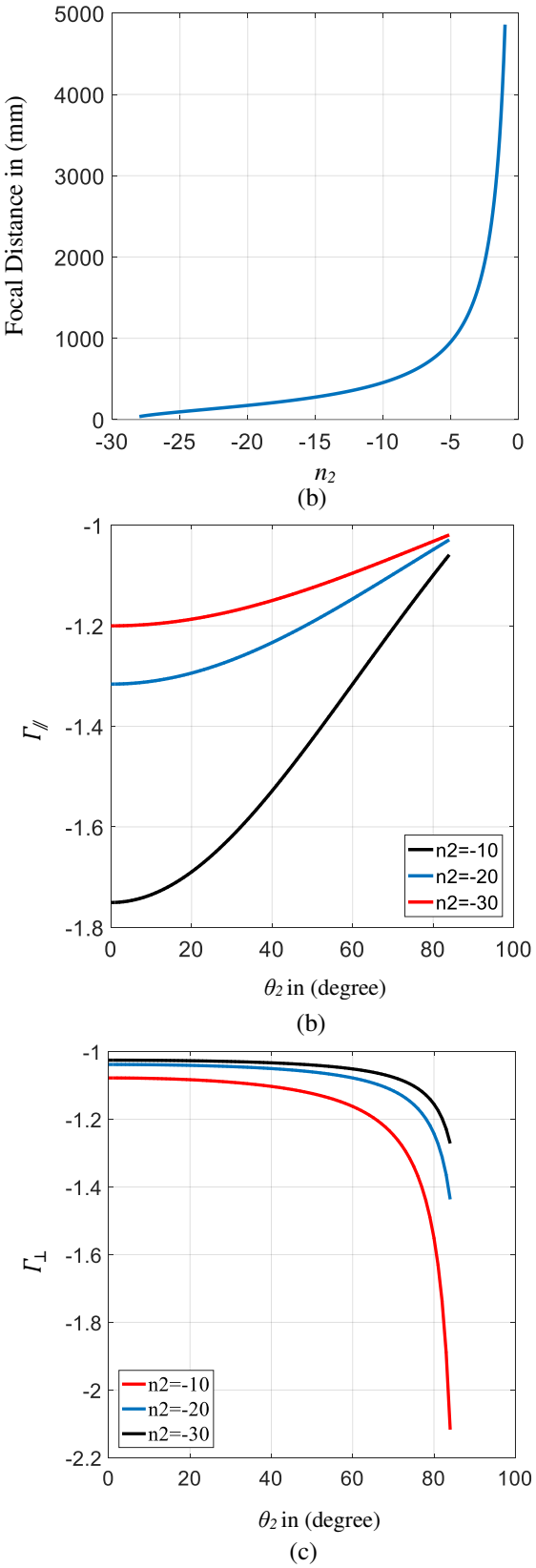

FIGURE 8. Calculated performances: (a) Focal distance F with respect to n_2, Reflection coefficients for n_2=-10, -20, and -30 at (b) parallel polarizations and (c) perpendicular polarizations.

VI. EBG UNIT CELL OPERATIONS

Now, the proposed unit cell electromagnetic properties are characterized analytically by using a transmission line model [22]. Such model is suggested by evaluating the equivalent circuit parameters model. Therefore, the equivalent circuit of the proposed EBG unit cell is presented in Fig. 9. The circuit is derived based on two main branches of a Left Hand (LH) branch and Right Hand (RH) branch to be a compose of LRHC. These branches are considered the representation of the LH and RH properties. The pin diodes are located at the middle of the unit cell to switch between the two branches by Logic_1 and Logic_0. Therefore, S-parameters should be evaluated based on the circuit model to realize a frequency resonance. Then, from the circuit model when the unit cell is switched ON, Logic_1, the unit cell should provide a well-defined frequency resonance. However, by switching the unit cell OFF, Logic_0, the frequency resonance must be disappeared from the entire frequency band of interest.

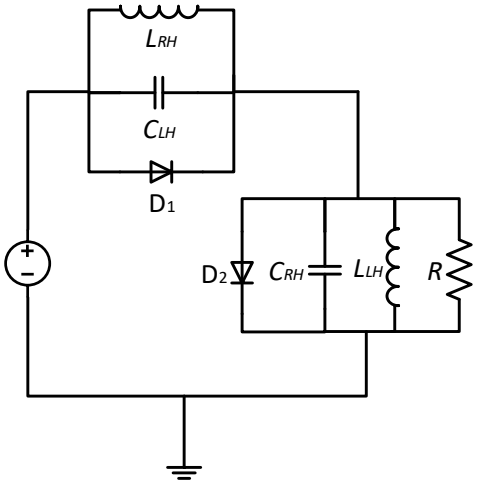

FIGURE 9. EBG unit cell equivalent circuit.

The proposed unit cell electromagnetic characterizations are tested numerically using CST MWS [24]. The EBG unit cell is positioned at the center of a virtual waveguide as shown in Fig. 10(a) to test the electromagnetic performance. The boundary conditions are selected as: the top and bottom sides (perpendicular on y-axis) are assigned as a Perfect Magnetic Conductors (PMC) while, the left and right sides (perpendicular on *x*-axis) are assigned as a Perfect Electric Conductors (PEC). TEM-modes are excited via two ports along z-axis as shown in Fig. 10(a). For this, Fig. 10(b) shows the simulated S_{11} and S_{12} for the two cases ON and OFF. It is important to mention that the authors decided to realize a resonant frequency for the unit cell at Logic_1 to 2.7 GHz for the design specifications [25]. It is found that the resonant frequency can be obtained for Logic_1 at 2.7 GHz. Nevertheless, in case of Logic_0, the frequency resonance is completely disappeared from the frequency band of interest. Therefore, the maximum power transfer can be obtained at logic_1 only, while, the power transfer would be shut off at logic_0 as will be proven later in this study.

Now, the lumped circuit elements are listed in Table III. These values are evaluated from the following two equations based on the geometrical dimensions of the unit cell [26]:

$$C_{RH} \approx \frac{0.264\,\epsilon_r + 0.3755}{ln\left(\frac{7.475\,F}{L_2}\right)} \qquad (7.A)$$

$$L_{RH} \approx ln\left(\frac{7.475\,F}{L_2}\right)^2 \qquad (7.B)$$

where, C_{RH} is mostly relative to the fringing capacitance that is calculated according to [26] which is independent of unit cell dimensions. The effect of the focal length on L_{RH} is realized significantly in equation (7.A) that is responsible on tuning the frequency resonance as will be seen later. *A* is the effective unit cell major dimension that is given by the physical unit cell length and the periodical gap to be about 60 mm. From the equivalent circuit model in Fig. 5, the frequency resonance f_r is given by equation (8).

$$f_r = \frac{1}{2\pi}\sqrt{\frac{L_{LH} + c_{LH}}{L_{LH}C_{LH}(L_{LR}+C_{LR})}} \qquad (8)$$

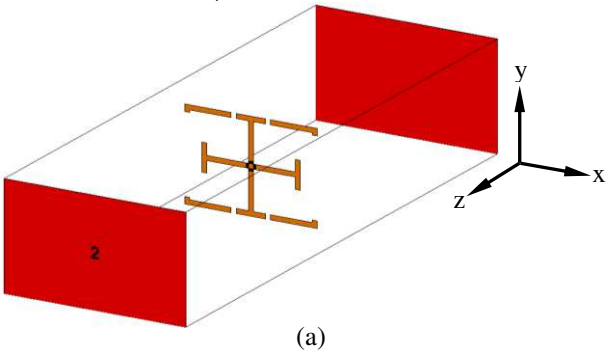

(a)

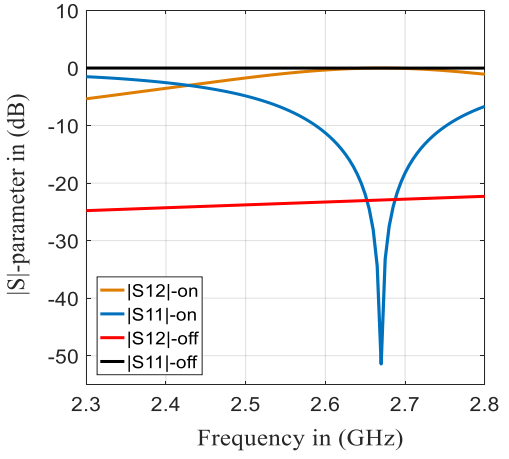

(b)

FIGURE 10. Unit cell performance characterizations (a) Numerical setup and (b) S-parameters.

TABLE III. EBG unit cell equivalent lumped elements.

parameter	*Value*
L_{LH}	*0.175 nH/m*
L_{RH}	*0.145 nH/m*
C_{LH}	*0.335 nF/m*
C_{RH}	*3.9 pF/m*
R	*50 Ω*

V. NUMERICAL STUDY

Fig. 11 shows the EBG-antenna structure design that is captured from the CSTMWS environments. The EBG layer is constructed from 5×5 array. The layer is mounted at distance of *d* from the patch structure. The optimal value of *d* is evaluated in this section numerically as will be seen later. As mentioned previously, the individual unit cell comes with four pin diodes and sharing the same ground plane for ASK modulation. The distance between the patch and the EBG layer represents the focal length *F* which is calculated from equation (4). The focal length is considered, about 70 mm, to maximize the antenna gain up to 10 dB as will be proven later. The patch structure is fed with a coaxial probe structure with a 50 Ω SMA port. The patch structure is slotted from the center with a cross geometry to achieve a hemispherical radiation pattern coverage [27]. The patch corners are terminated to enhance the matching impedance [28].

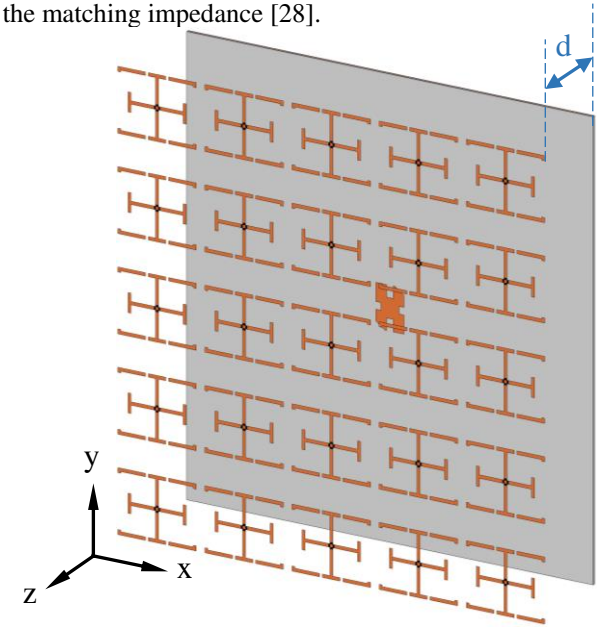

FIGURE 11. Reconfigurable EBG layer with the antenna structure.

Now, CST MWS simulations are invoked to study the best EBG location, array size, and orientation with respect to the microstrip patch antenna. Therefore, to establish such a study, the authors started with initial guesses are calculated based on the analytical study that was presented in section III. By changing the EBG array configuration size from 1×1, 3×3, 5×5, and 7×7, the antenna gain is found to be significantly changing as seen in Fig. 12. On the other hand, it is found with increasing the EBG layer size, the side and back lobs are reduced significantly. These observations are attributed to the TIR of the coming rays is reduced significantly with increasing the array size [11]. Nevertheless, the refracted rays that are presented by the diffraction from the array edges are significantly vanished with increasing the array size. Thus, by returning back to equation (5), we find the gain is significantly affected with the location of the antenna from the EBG layer that is presented by *F* and the EBG size that is given by *W*.

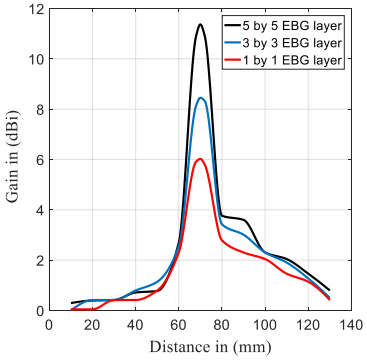

FIGURE 12. Antenna performance variation with a parametric study.

In another aspect, Fig. 13 shows E-fields and current surface distributions of the proposed EBG layer for both logic_1 and logic_0 cases. In general, it is found that the proposed EBG layer shows asymmetrical E-fields and surface current distributions along the *x*- and *y*-planes due to the asymmetrical unit cell geometry along *x*- and *y*-planes. This realizes the phenomena of stigmatism effects [14]; which effects on the radiation patters as will be seen later. Nevertheless, in case of logic_0, E-field is reached in maximum up to 600 V/m, see Fig. 13(a); however, in case of logic_1, the E-filed is elevated around 2000 V/m as presented in Fig. 13(c). This enhancement in the E-field is achieved by the resonance at 2.45 GHz for logic_1; which removes the reactive impedance parts to realize the maximum power transfer radiation [29]. Moreover, the same observation is noticed in the surface current distributions for both cases: logic_1 and logic_0 that are seen in Figs. 13(b) and 13(d). It is found that the proposed EBG layer surface current distribution at logic_0 is almost 0.2 A; however, it is enhanced up to 7 A for logic_1. Such that convey our theory of having the maximum power transfer when the EBG layer works at the resonance as in case logic_1; which is not similar to the logic_0 case.

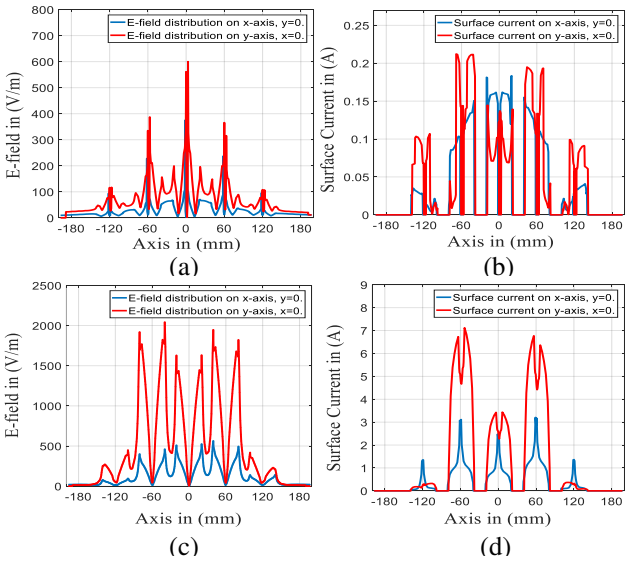

FIGURE 13. E-Fields and surface current distributions of the proposed EBG layer; (a) E-Field at logic_0, (b) surface current at logic_0, (c) E-Field at logic_1, and (d) surface current at logic_1.

VI. MEASUREMENTS AND VALIDATION

After the arriving to the optimal antenna design numerically, the authors attempted the antenna fabrication as seen in Fig. 14. The antenna is fabricated based on a chemical etching process of the PCB technology. The EBG layer is mounted on four ballistic screws as seen in Fig. 15. The length of each screw is 70 mm. It is good to mention, that the fabricated EBG layer is not soldered to the pin diodes due to the fabrication limitations. Moreover, the aim of this study is to avoid any consequences errors due to the diodes biasing including the wiring and soldering. Therefore, for logic_1 case, the positions of the pin diodes are shorted with copper stripes. However, another layer is fabricated for logic_0 case without shorting the places of the pin diodes to emulate the open circuit case.

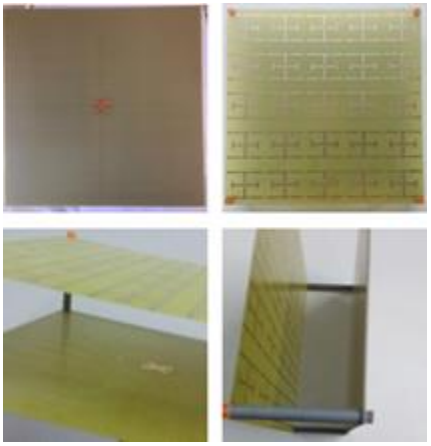

FIGURE 14. Fabricated antenna and the EBG-layer.

The antenna performance in terms of S_{11} spectra, gain, spectra, and radiation patterns are measured using a typical measurement system. The used system is based on coaxial cables, vector network analyzer of Agilent PNA 8720 series, and 82357A USB to GPIB interface that is connected to an external computer. The antenna is placed on a rotational holder inside an RF anechoic chamber as seen in Fig. 15.

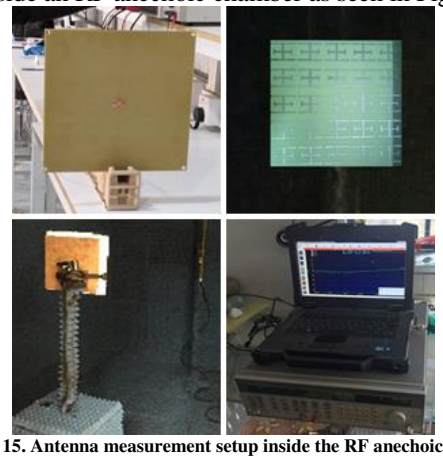

FIGURE 15. Antenna measurement setup inside the RF anechoic chamber.

The simulated and measured S_{11} spectra as well as the obtained gain values over the frequency range, (2.3-2.55) GHz, are shown in Fig.16. At first, Fig. 16(a) represents S_{11} and gain spectra for the antenna without EBG layer. The maximum antenna gain is found at 2.45 GHz about 1 dBi. Next, the spectra of S_{11} and gain for the antenna based EBG layer with logic_0 case are shown in Fig. 16(b); it is found the antenna provides a resonance frequency of 2.45 GHz with gain of 2 dBi. The final set of measurements is presented in Fig. 16(c) for the antenna based EBG layer of logic_1. It is found that the antenna shows a gain of 11 dBi at 2.45 GHz.

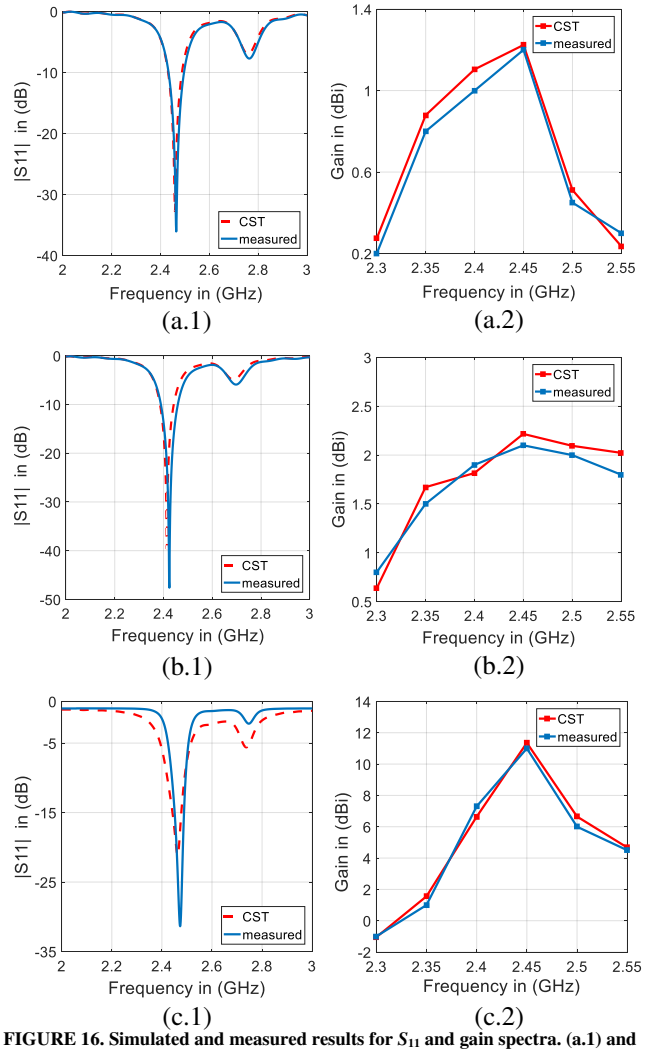

FIGURE 16. Simulated and measured results for S_{11} and gain spectra. (a.1) and (a.2) S_{11} and gain spectra for antenna without EBG layer. (b.1) and (b.2) S_{11} and gain spectra for antenna with EBG layer based logic_0. (c.1) and (c.2) S_{11} and gain spectra for antenna with EBG layer based logic_1.

Next, the presented results in Fig. 17 show a comparison between the measured and simulated radiation patterns at two perpendicular planes at ϕ=0° and ϕ=90°. It is proven at first; an excellent agreement is achieved between the simulated and measured results. Next, it is found the antenna radiation pattern, without the EBG layer, covers a wide beam width of 136° with gain of 1 dBi as seen in Fig. 17(a). Later, in Fig. 17(b), the antenna beam width is reduced to 100° to achieve higher gain of 2 dBi for the case of antenna based EBG layer with logic_0. The antenna based on EBG layer for logic_1, the antenna gain is enhanced significantly to 11 dBi with a narrow beam width

of 19° as depicted in Fig. 17(c). Moreover, it is obvious from the achieved results, the antenna in case of logic_1 with EBG layer shows more symmetrical main lobe beam than other cases. This is attributed to the ability of the proposed EBG layer for correcting the antenna radiation pattern through the stigmatism effects [14].

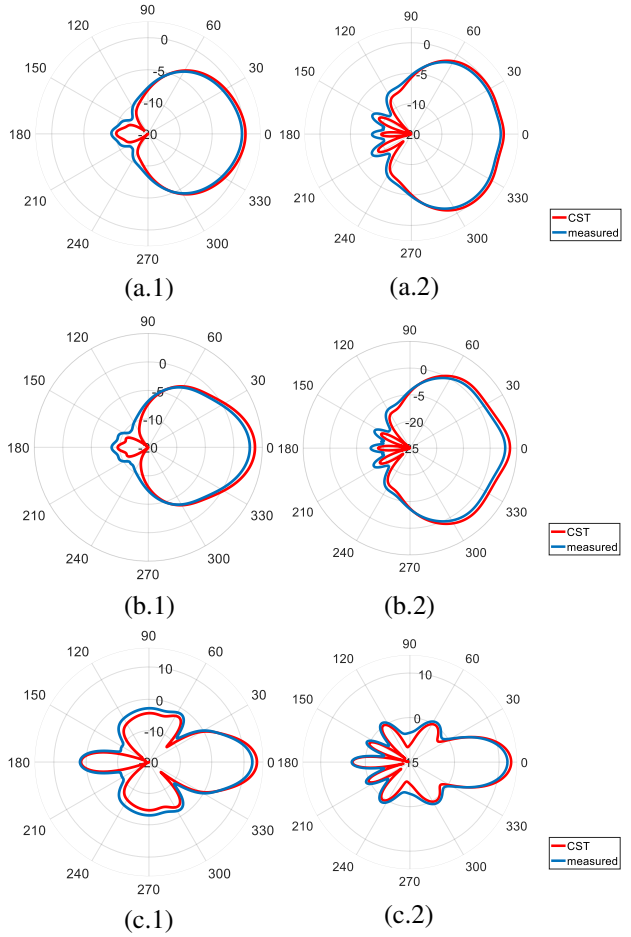

FIGURE 17. Radiation patterns based simulated and measured results for the proposed antenna: (a.1) and (a.2) without the EBG layer at ϕ=0° and ϕ=90°, respectively. (b.1) and (b.2) with the EBG layer for logic_0 case at ϕ=0° and ϕ=90°, respectively. (c.1) and (c.2) with the EBG layer for logic_1 at ϕ=0° and ϕ=90°, respectively.

Experimentally, in terms of the total efficiency, the proposed antenna shows a total efficiency of 20 % when it is considered without EBG introduction. However, adding the EBG layer with logic_0 statues; the total efficiency is improved to 48 %. A further enhancement is achieved after adding the EBG layer with logic_1 statues to reach 95 %. The reason of such improvements in the total efficiency, at logic_1 case, the EBG layer shows a frequency resonance at which the total impedance reactive part becomes zero. Therefore, most the power is transferred through the EBG layer which is converted to real power without conservation in the storage elements [30] as also explained later in section IV. Furthermore, the authors conducted their study to the antenna parameters variation which changing the proposed EBG layer orientation with respect to the patch. The proposed EBG layer is oriented around the x-y plane center. The aim of such study is to realize the effects of the EBG unit cell asymmetry on the antenna gain. As summarized in table IV, it is found by orienting the EBG layer from 90° to 0°, when the EBG is switched ON at logic_1, the antenna gain is enhanced from 10 dBi to 11dBi. However, for case logic_0, the antenna gain is found to be 2 dBi at 0° and 2.6 dBi at 90°. This is attributed to the stigmatism effects in the proposed EBG layer as explained in section III; that is considered a correction factor in such case. Therefore, the authors decided to consider the 0° orientation is the optimal case that realizes a gain difference between logic_0 and logic_1 statues about 9 dBi that is very suitable for ASK modulation process. The front to back ratio (*f/b*) is found to be insignificantly changed by orienting the EBG layer from 0° to 90°.

TABLE IV. EBG layer rotation effects on the antenna performance.

at orientation = 0°						
State	*f_r (GHz)*	*S_{11} (dB)*	*Gain (dBi)*	*f/b*	*Tot. eff.*	*Rad. eff.*
OFF	*2.42*	*-39*	*2*	*7.5*	*28%*	*29%*
ON	*2.42*	*-21*	*11*	*5.2*	*44%*	*45%*
at orientation = 90°						
state	*f_r (GHz)*	*S_{11} (dB)*	*Gain (dBi)*	*f/b*	*Tot. eff.*	*Rad. eff.*
OFF	*2.41*	*-40*	*2.6*	*7.4*	*28%*	*29%*
ON	*2.41*	*-25*	*10*	*6.5*	*39%*	*39%*

Finally, the proposed antenna system performance is compared to other published results in table V. It is found that the proposed antenna shows excellent gain difference by showing excellent controllability in the EBG layer performance in comparison to other published results.

TABLE V. The proposed work enhancement comparison with respect to other published results.

Reference	*f_r (GHz)*	*Subst.*	*Size (mm^2)*	*Gain (G) or Directivity (D) enhancement (dBi)*
[12]	*2.45*	*FR4*	*240×240*	*G=5.1*
[14]	*2.65*	*Taconic*	*360×360*	*G=7.8*
[15]	*5.8*	*FR4*	*50×50*	*G=1.2*
[16]	*11.38*	*ϵ_r =3.5*	*50×50*	*D=7.88*
[17]	*9.6*	*RO3003*	*63×63*	*D= 6*
[31]	*5.2*	*FR4*	*50×50*	*G=4.54*
proposed work	*2.45*	*FR4*	*294×294*	*G=10, D=9*

VII. CONCLUSION

At the end, we have proposed a new strategy based on DAM process to design an ASK digital metasurface. The proposed antenna system at switching the EBG layer ON, logic_1, provides a gain of 11 dBi and when the EBG layer is switched OFF, logic_0, the gain drops down to 2 dBi in relative to sequences cyclical of the modulation period. By switching all unit cells in the EBG layer electronically; digital coding can control the transmitted electromagnetic power from the proposed antenna system. The principle of operation of the proposed EBG layer based on optical raytracing analysis is

proven as well as the equivalent circuit model. By the raytracing analysis, we demonstrated that the focused antenna beam, the antenna beam width, at the resonant frequency is significantly affected by the EBG layer refractive index. The EBG layer refractive index is found mainly related to the EBG effective capacitive variation as proven in the circuit model. Moreover, the effect of angle of incidence with respect to the proposed EBG layer is discussed in terms of TIR. It is found that the EBG introduction could be a significant cause of side lobes generation. This is attributed to the beam reflection at the critical angle of incidence. Since, the antenna gain mainly dependences on the emerged beam width which in turns relative to the EBG focal length, switching the EBG layer is found to vary the total effective value of the capacitive part in the EBG. Therefore, the authors realized an excellent control process on the antenna gain through switching the EBG layer. An EBG prototype is fabricated and experimentally characterized to validate the proposed analysis, which indicates excellent agreement with the numerical results. Another interesting achievement, it is found by rotating the EBG layer with 90º in respect to the normal axis on the patch antenna, a significant variation could be achieved in the radiation pattern and gain. Such phenomenon is explained in the paper based on the effects of stigmatism apparition that is discovered from mongering the field distribution on the EBG layer. Therefore, it is found that the EBG layers can be designed in such way to correct the impinging radiation patterns from antennas to characterize well symmetric main lobes as achieved in our proposed antenna system. Moreover, it is found that in case of switching the EBG layer OFF, the amount of the generated surface current is much less than the surface current amount in case of switching the EBG layer ON. For the E-fields the case is found the same, this is attributed to the dispersing the EBG resonance in case of logic_0 that converts most the radiated power to a conservative reactive part between the antenna patch and the EBG layer. However, in case of having logic_1 at which the resonance is taken place, most the power is lacked smoothly where it is converted to a real part. Finally, the antenna system radiation efficiency is found to be significantly enhanced by switching the EBG layer ON due to the fact of having total impedance reactive part is zero at resonance.

REFERENCES

[1] I. Glover and P. Grant, “Bandpass modulation of a carrier signal,” in *Digital Communications*, 3rd ed., England: Prentice Hall, 2010, pp. 390-449.

[2] S. Henthorn, K. L. Ford and T. O’Farrell, "Bit-Error-Rate Performance of Quadrature Modulation Transmission Using Reconfigurable Frequency Selective Surfaces," *IEEE Antennas Wireless Propag. Lett*, vol. 16, pp. 2038-2041, 2017.

[3] A. Babakhani, D. B. Rutledge and A. Hajimiri, "Transmitter Architectures Based on Near-Field Direct Antenna Modulation," *IEEE Journal of Solid-State Circuits*, vol. 43, no. 12, pp. 2674-2692, Dec. 2008.

[4] D. Park, M. Kim and D. Cho, "Novel Single-RF MIMO System Based on Repetitive Pulse Width Modulation," *IEEE Communications Lett.,* vol. 20, no. 1, pp. 165-168, Jan. 2016.

[5] M. Manteghi, “A wideband electrically small transient-state antenna,” *IEEE Trans. Antennas Propag.*, vol. 64, no. 4, 2016, pp.1201–1208.

[6] G. Kiani, and T. Bird, “ASK modulator based on switchable FSS for THz applications,” RADIO SCIENCE, vol. 46, no. 2, pp. 1-8, Apr. 2011.

[7] S. Henthorn, K. Ford, and T. O’Farrell, “Frequency Selective Surface Loaded Antenna for Direct Antenna Modulation,” *Proc. On Antennas and Propagation (EUCAP),* Paris, France, pp. 731-734, Mar. 2017.

[8] Ahmed H. Abdelrahman, Fan Yang, Atef Z. Elsherbeni, and Payam Nayeri, “Space-fed Array Design Method,” in Analysis and Design of Transmitarray Antennas, 1st ed., San Rafael, California, USA: Morgan & Claypool, pp. 7–8, 2017.

[9] Constantine A. Balanis, “Fundamental Parameters and Figures-of-Merit of Antennas,” in *ANTENNA THEORY ANALYSIS AND DESIGN*, 4th ed., Hoboken, New Jersey, USA: Wiley & Sons, pp. 63–64, 2016.

[10] A. Babakhani, D. B. Rutledge, and A. Hajimiri, “Transmitter architectures based on near-field direct antenna modulation,” Solid-State Circuits, IEEE Journal of, vol. 43, no. 12, pp. 2674–2692, 2008,

[11] Y. Al-Naiemy, T. A. Elwi, and N. Lajos, “Enhancing the Microstrip Antenna Gain Using a Novel EBG Lens Based on a Single Layer”, Proceedings of the 3rd Colloquium on Microwave Communication, Aug. 2018.

[12] Y. Alnaiemy, T. A. Elwi, N. Lajos, and T. Zwick, “A Systematic Analysis and Design of a High Gain Microstrip Antenna based on a Single EBG Layer,” IEEE INFOCOMMUNICATIONS JOURNAL, volume 10, pp. 1-9, December, 2018.

[13] T. A. Elwi, H. M. Al-Rizzo, N. Bouaynaya, M. M. Hammood, and Y. Al-Naiemy, “Theory of gain enhancement of UC–PBG antenna structures without invoking Maxwell’s equations: an array signal processing approach,” Progress In Electromagnetics Research B, volume 34, pp. 15-30, August 2011.

[14] T. A. Elwi, H. M. Al-Rizzo, D. G. Rucker, F. Song, “Numerical simulation of a UC–PBG lens for gain enhancement of microstrip antennas,” International Journal of RF and Microwave Computer-Aided Engineering, volume 19, issue 6, pp. 676–684, Nov. 2009.

[15] R. V. Sravya and R. Kumari, "Gain enhancement of patch antenna using L-slotted mushroom EBG," *2018 Conference on Signal Processing And Communication Engineering Systems (SPACES)*, Vijayawada, 2018.

[16] Yongxing Che, Xinyu Hou and Peng Zhang, "Design of multiple FSS screens with dissimilar periodicities for directivity enhancement of a dual-band patch antenna," *Proceedings of the 9th International Symposium on Antennas, Propagation and EM Theory*, Guangzhou, 2010.

[17] A. Pirhadi, H. Bahrami and J. Nasri, "Wideband High Directive Aperture Coupled Microstrip Antenna Design by Using a FSS Superstrate Layer," *IEEE Trans. Antennas Propag.,* vol. 60, no. 4, pp. 2101-2106, Apr., 2012.

[18] Kodera, "Smart metasurface with non-reciprocity for Fog layer in IoT environment," *IEEE International Symposium on Electromagnetic Compatibility and 2018 IEEE Asia-Pacific Symposium on Electromagnetic Compatibility (EMC/APEMC)*, Singapore, pp. 912-914, 2018.

[19] L. Liu, L. Kang, T. S. Mayer, and D. H. Werner, “Hybrid metamaterials for electrically triggered multifunctional control,” *Nature Comm.,* vol. 7, no. 1, 2015.

[20] P. Hosseini, C. D. Wright, and H. Bhaskaran, “An optoelectronic framework enabled by low-dimensional phase-change films,” Nature, vol. 511, no. 7508, pp. 206–211, 2014.

[21] Y. Yao, R. Shankar, M. A. Kats et al., “Electrically tunable metasurface perfect absorbers for ultrathin mid-infrared optical modulators,” Nano Letters, vol. 14, no. 11, pp. 6526–6532, 2014,

[22] T. A. Elwi, D. A. Jassim, H. H. Mohammed, “Novel miniaturized folded UWB microstrip antenna-based metamaterial for RF energy harvesting,” *International Journal of Communication Systems*, Volume 1, issue 2, January 2020.

[23] Z. Al-Dulaimi, T. A. Elwi, and D. C. Atilla, “Design of a Meander Line Monopole Antenna Array Based Hilbert-Shaped Reject Band Structure for MIMO Applications,” *IETE Journal of Research*, Volume 66, issue 1, pp. 1-10, Mar., 2020.

[24] CST Microwave Studio, [online] Available at: http:www.cst.com [Accessed: 28 May 2018].
[25] T. A. Elwi, “Printed Microwave Metamaterial-Antenna Circuitries on Nickel Oxide Polymerized Palm Fiber Substrates,” *Nature Scientific Reports,* volume 9, number 2174, pp. 1-14, Jan. 2019.
[26] T. A. Elwi, Z. A. AL-Hussain, O. Tawfeeq, “Hilbert Metamaterial Printed Antenna based on Organic Substrates for Energy Harvesting”, *IET Microwaves, Antennas & Propagation*, volume 12, number 4, pp.1-8, Jun. 2019.
[27] H. M. Al-Rizzo, K. G. Clark, J. M. Tranquilla, R. A. Adada, T. A. Elwi, and D. Rucker, “Enhanced low-angle GPS coverage using solid and annular microstrip antennas on folded and drooped ground planes,” IEEE Transaction on Antenna and Propagation, volume 57, number 11, November 2009.
[28] S. Chaimool, K. L. Chung, and P. Akkaraekthalin, "Simultaneous Gain and Bandwidths Enhancement of a Single-Feed Circularly Polarized Microstrip Patch Antenna Using a Metamaterial Reflective Surface," Progress In Electromagnetics Research B, volume 22, pp. 23-37, May 2010.
[29] H. S. Ahmed and T. A. Elwi, “On the design of a reject band filter for antennas mutual coupling reduction”, International Journal of RF and Microwave Computer-Aided Engineering, volume 11, number 3, pp.1-11, April 2019.
[30] H. M. Al-Sabbagh, T. A. Elwi, Y. Al-Naiemy, and H. M. Al-Rizzo, “A Compact Triple-Band Metamaterial-Inspired Antenna for Wearable Applications”, *Microwave and Optical Technology Lett.*, volume 11, number 2, May 2019.
[31] A. Mellita, D. S. Chandu and S. S. Karthikeyan, "Gain enhancement of a microstrip patch antenna using a novel frequency selective surface," *2017 Twenty-third National Conference on Communications (NCC)*, Chennai, 2017.

Hayder Almizan received B.S. degree in electrical engineering from University of Kufa, Najaf, Iraq, in 2008 and Higher Diploma degree in aerospace engineering from the Sapienza University of Rome, Rome, Italy, in 2014. He is currently pursuing his M.Sc. degree in electronics and communications engineering at Mustansiriyah University, Baghdad, Iraq. From 2009 to 2012, he worked at the consultant engineering department of Kufa University. Since 2014, he joined the electronics and communications engineering department in Kufa University. His recent research interests include signal processing, neural network, numerical techniques for electromagnetic engineering of metamaterials and artificial structures.

Taha A. Elwi received his B.Sc. in Electrical Engineering Department (2003) (Highest Graduation Award), Postgraduate M.Sc. in Laser and Optoelectronics Engineering Department (2005) (Highest Graduation Award) from Nahrain University Baghdad, Iraq. From April 2005 to August 2007, he was working with Huawei Technologies Company, Baghdad, Iraq. On January, 2008, he joined the University of Arkansas at Little Rock and he obtained his Ph.D. in December 2011 from the system engineering and science. His research areas include wearable and implantable antennas for biomedical wireless systems, smart antennas, Wi-Fi deployment, electromagnetic wave scattering by complex objects, design, modeling and testing of metamaterial structures for microwave applications, design and analysis of microstrip antennas for mobile radio systems, precipitation effects on terrestrial and satellite frequency re-use communication systems, effects of the complex media on electromagnetic propagation and GPS. The nano-scale structures in the entire electromagnetic spectrum are a part of his research interest.

Zaid Asaad Abdul Hassain was born in Baghdad, Iraq, in 1979. He received the B.S. and the M.S. degree from the AL-Mustansiriyah University, Faculty of Engineering, Electrical Engineering Department, Iraq, in 2000 and 2003, respectively. His research interests include microwave and antenna.

Figures

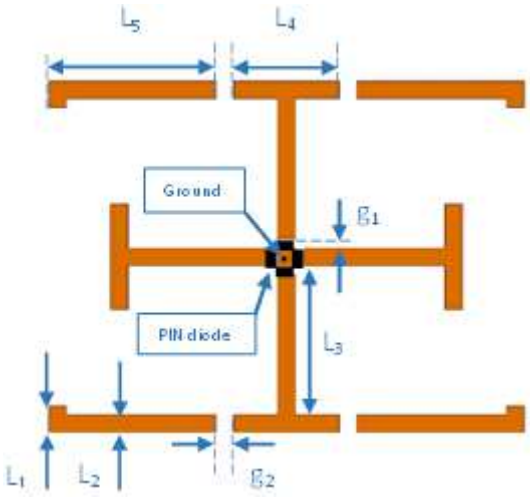

Figure 1

EBG unit cell structure.

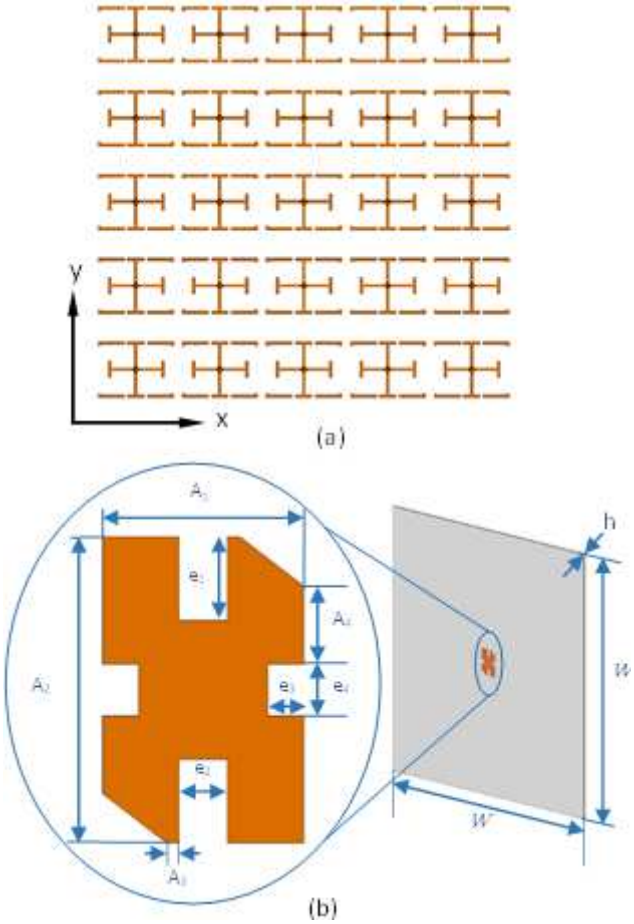

Figure 2

The proposed antenna structure; (a) EBG structure and (b) Microstrip antenna.

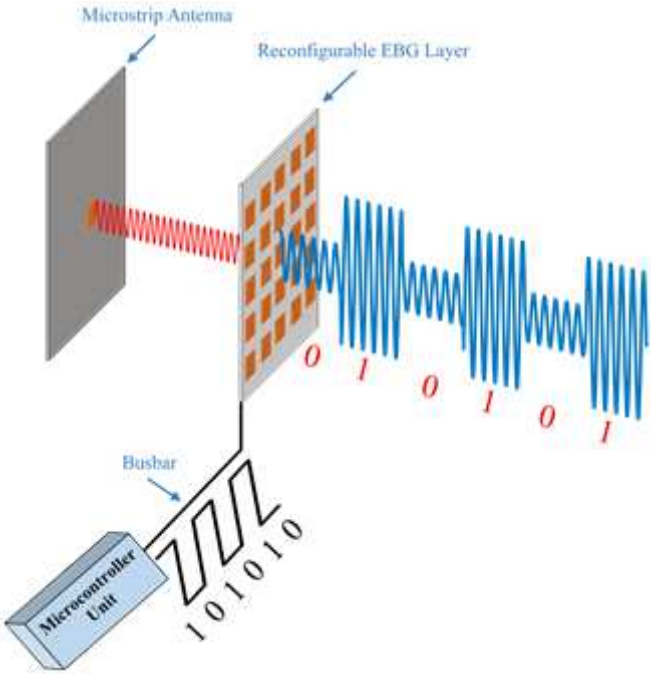

Figure 3

System schematic of the proposed ASK modulator.

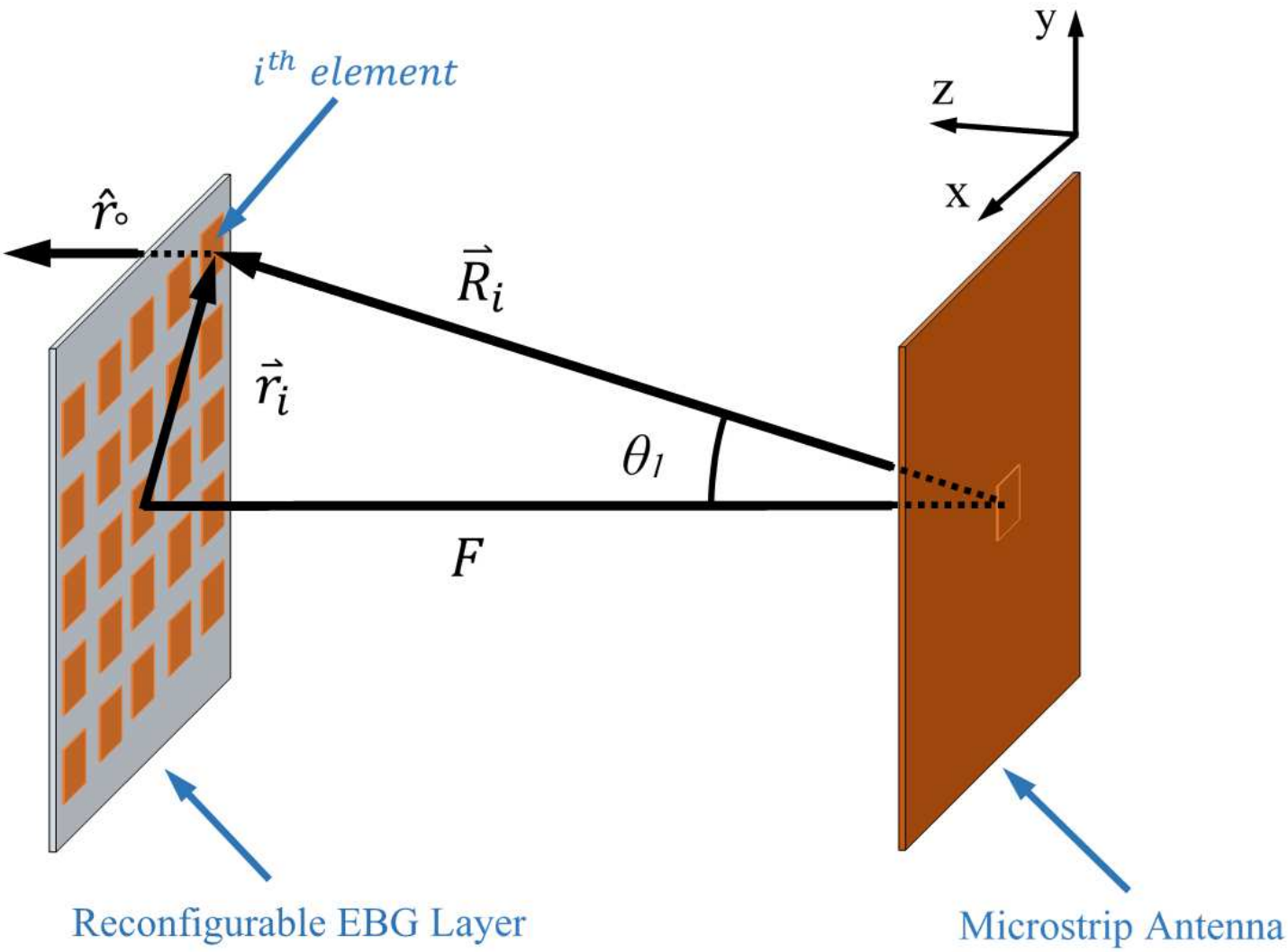

Figure 4

Ray tracing based phase difference.

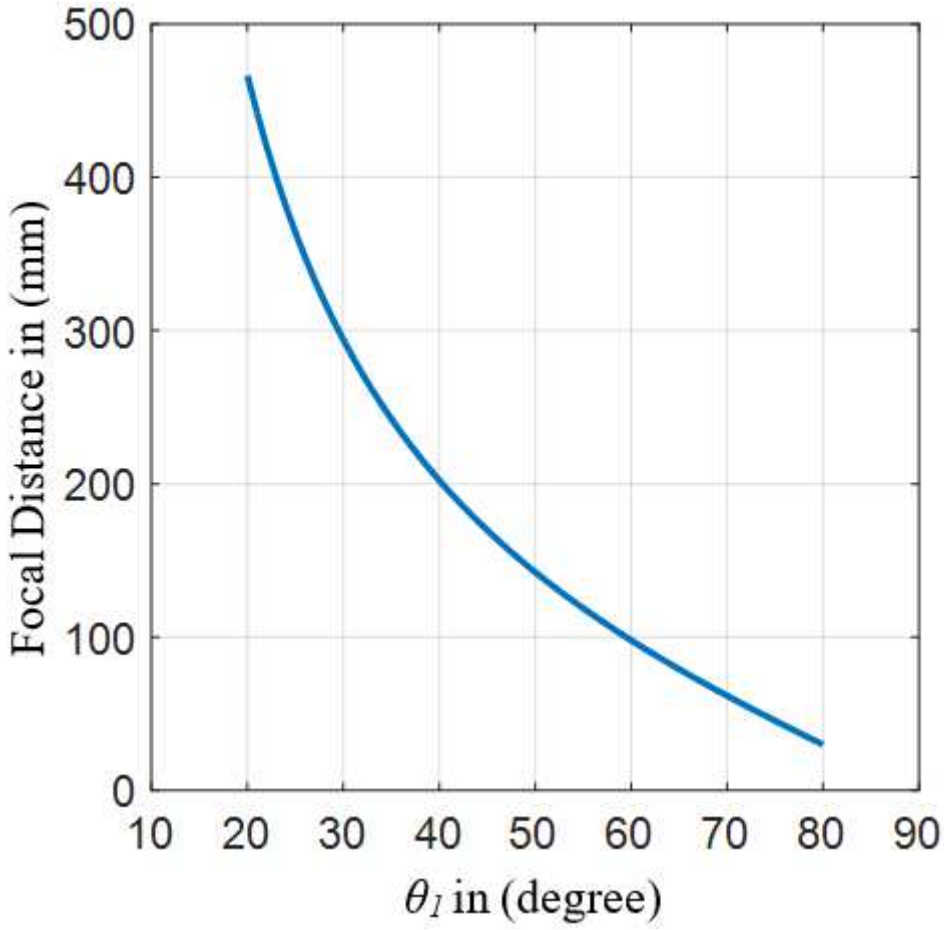

Figure 5

Ray tracing analysis.

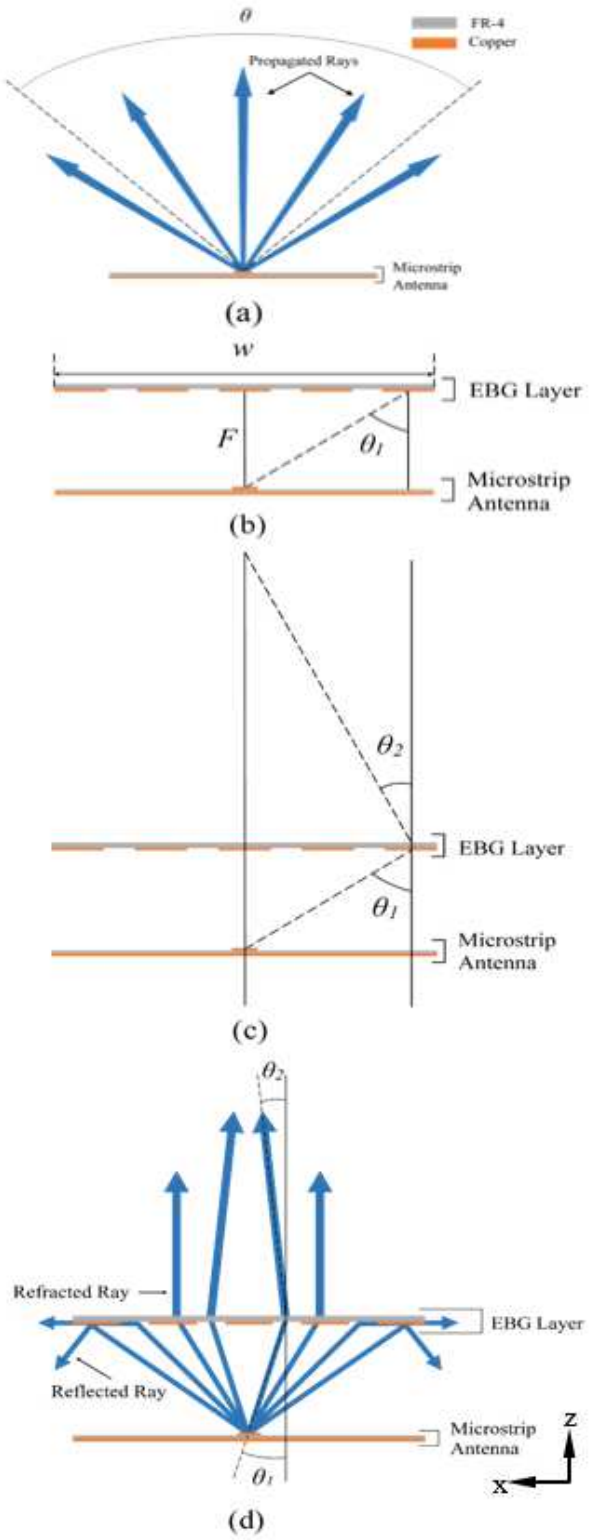

Figure 6

Ray tracing analysis; (a) diverging beams from the antenna, (b) extreme beams incidence, (c) beam refraction, and (d) total internal reflection.

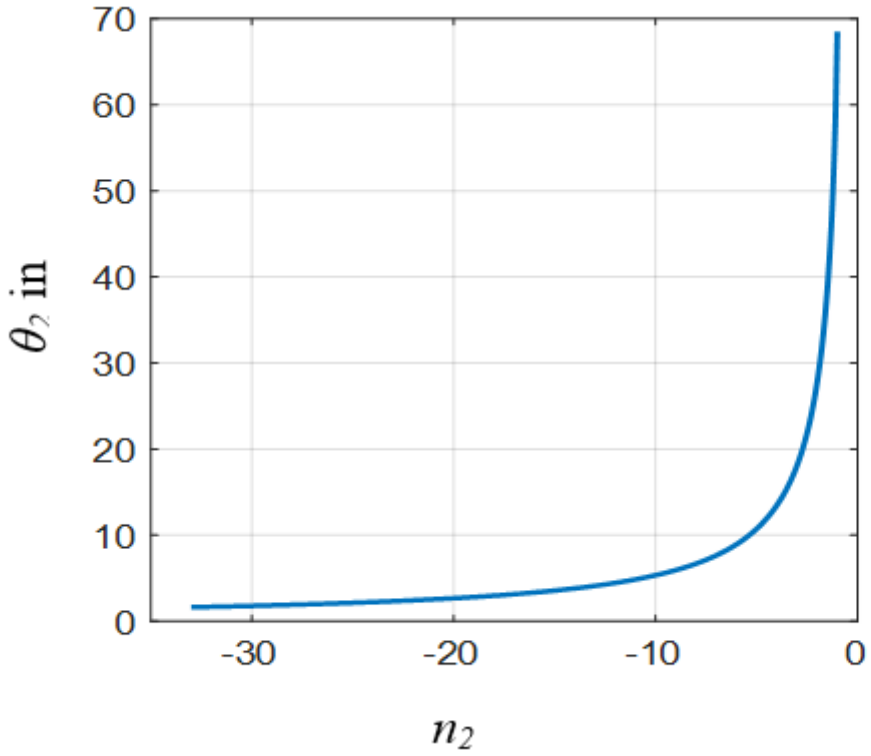

Figure 7

Changing of θ2 with respect to n2 according to Snell's law.

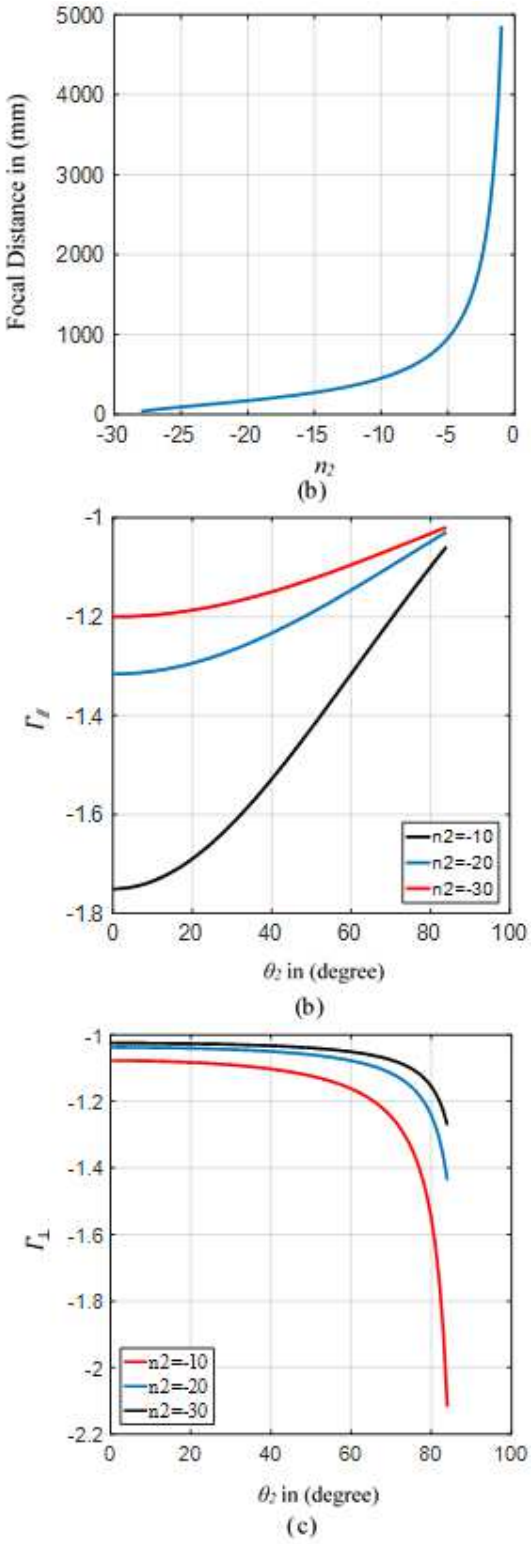

Figure 8

Calculated performances: (a) Focal distance F with respect to n2, Reflection coefficients for n2=-10, -20, and -30 at (b) parallel polarizations and (c) perpendicular polarizations.

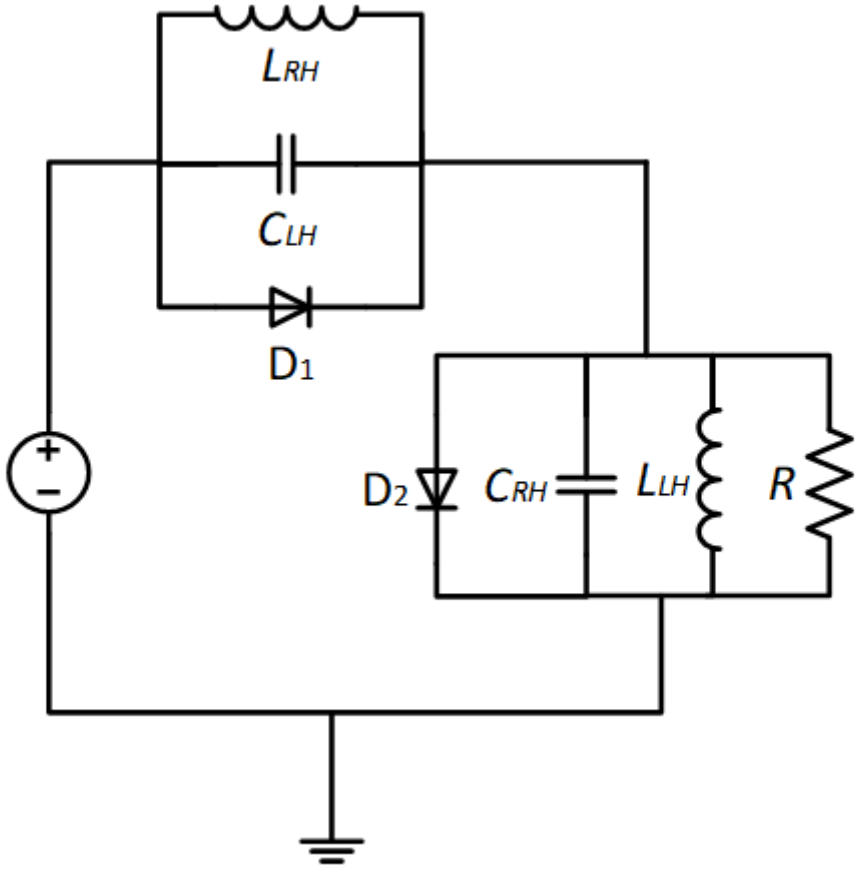

Figure 9

EBG unit cell equivalent circuit.

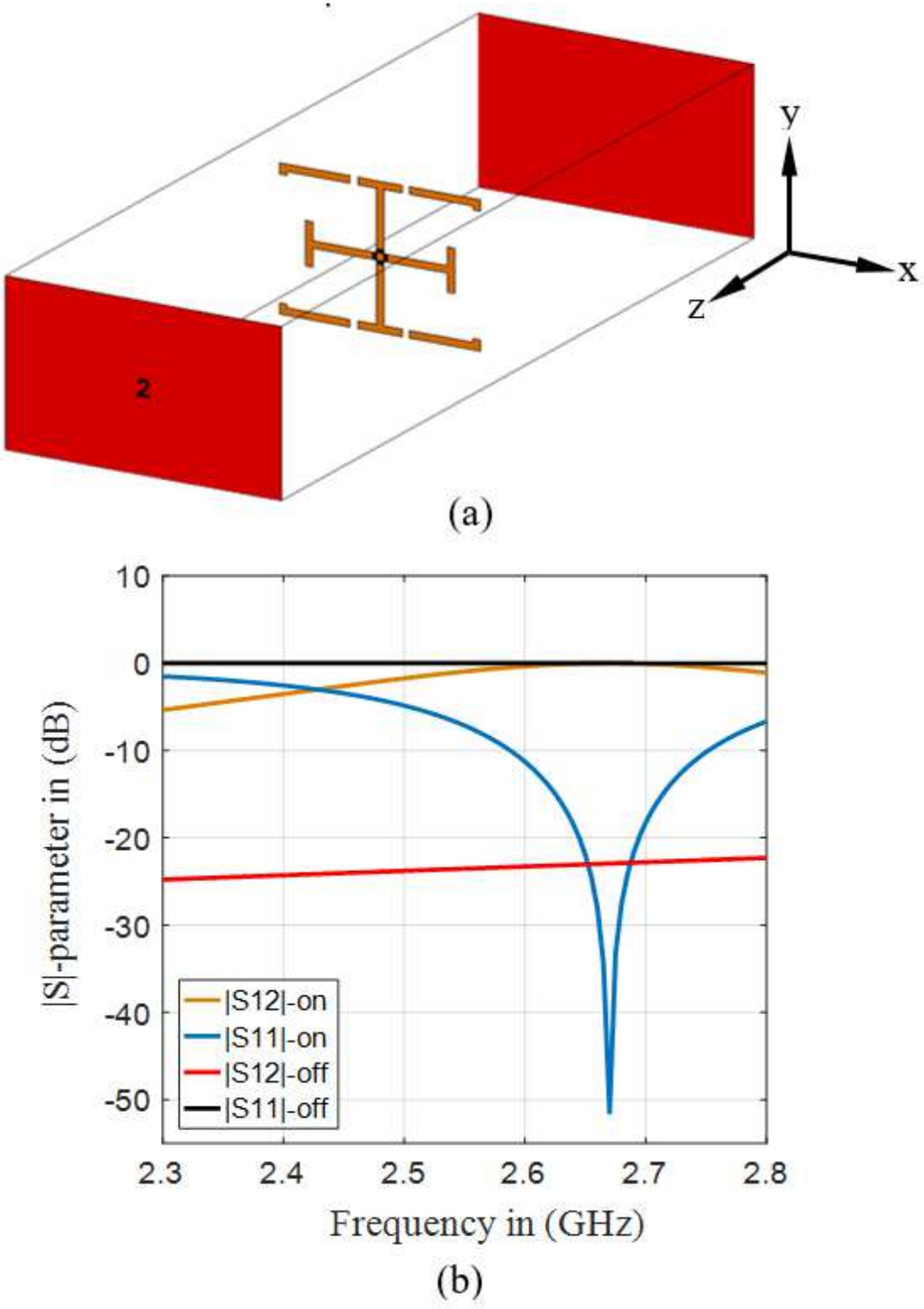

Figure 10

Unit cell performance characterizations (a) Numerical setup and (b) S-parameters.

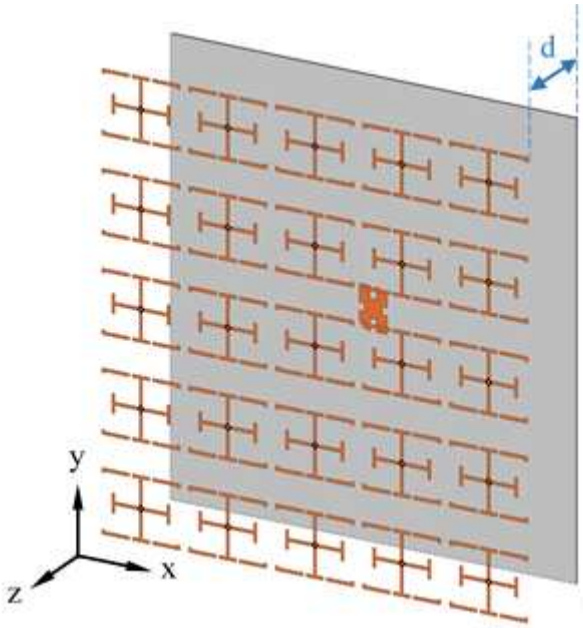

Figure 11

Reconfigurable EBG layer with the antenna structure.

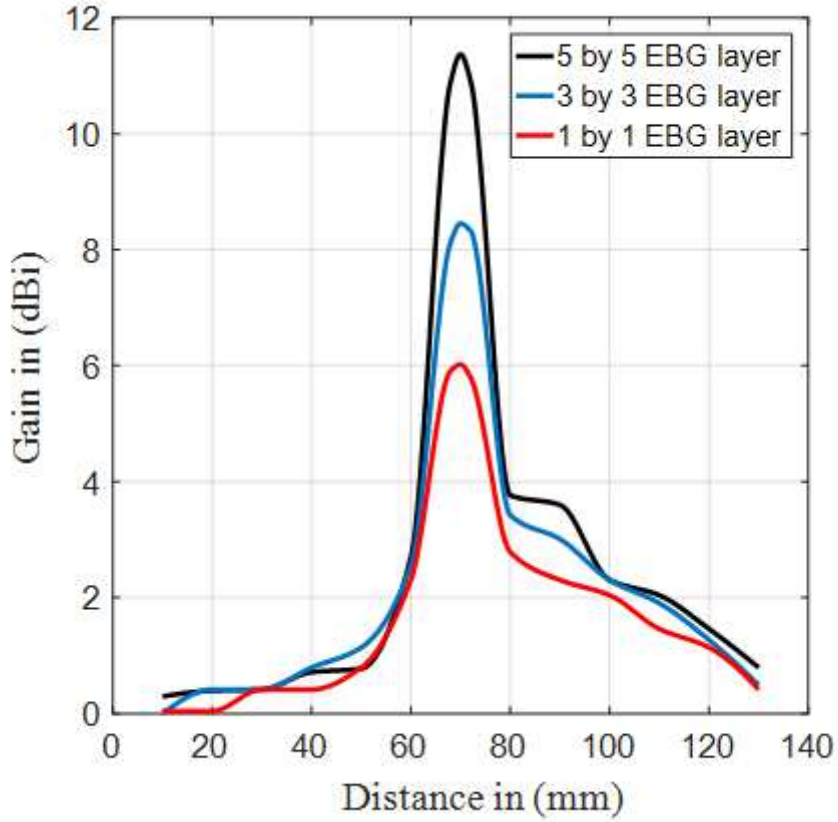

Figure 12

Antenna performance variation with a parametric study.

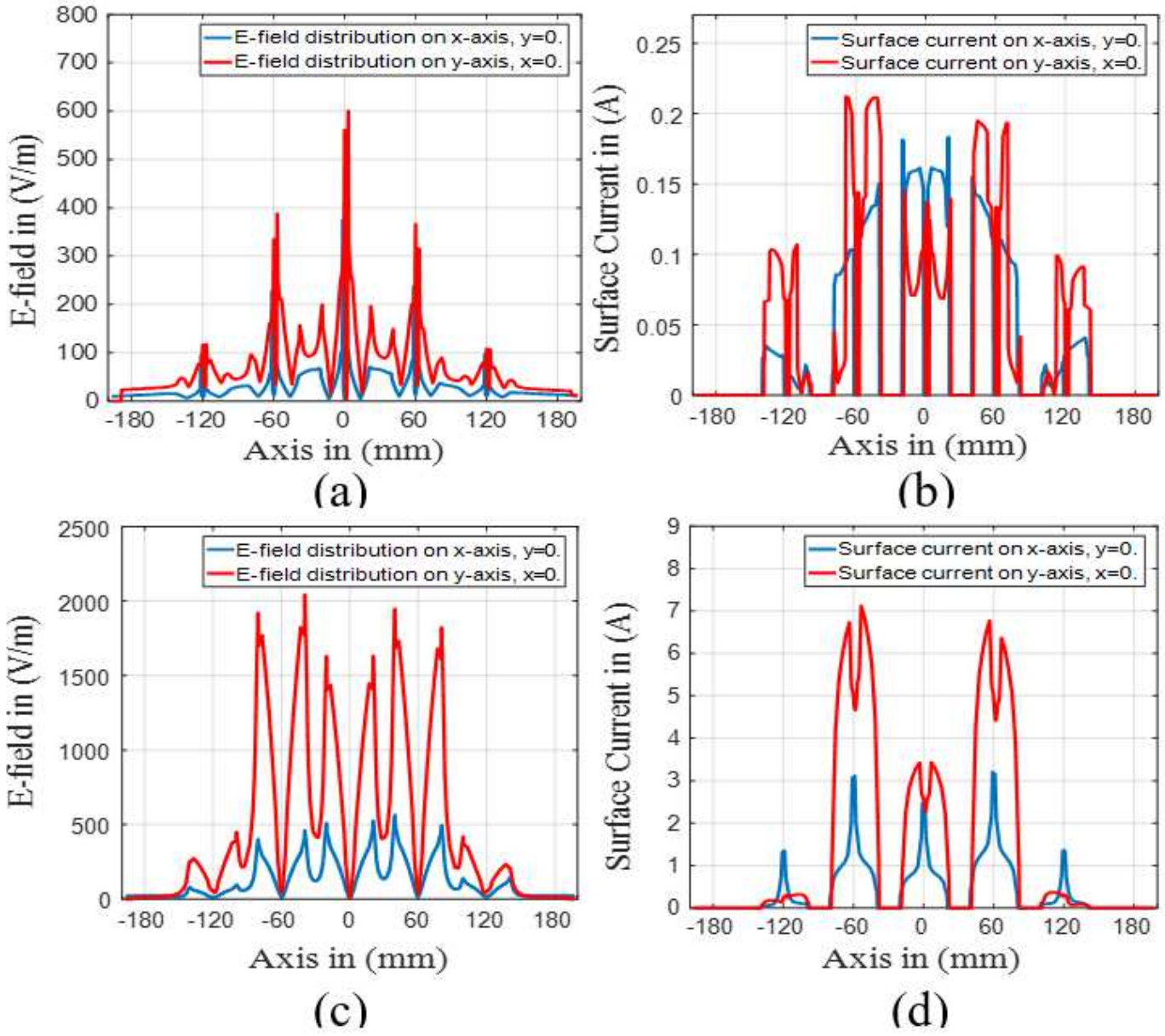

Figure 13

E-Fields and surface current distributions of the proposed EBG layer; (a) E-Field at logic_0, (b) surface current at logic_0, (c) E-Field at logic_1, and (d) surface current at logic_1.

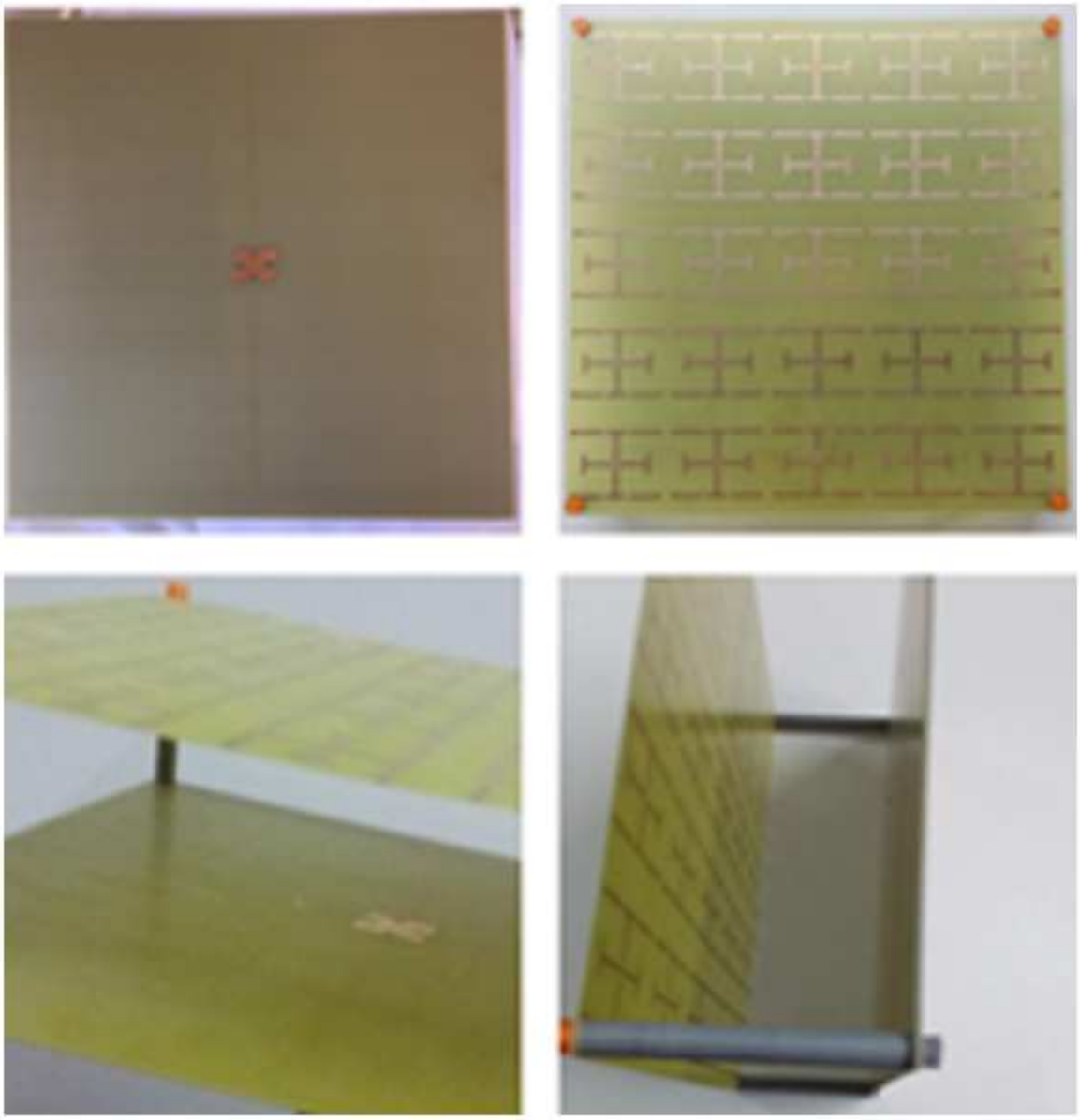

Figure 14

Fabricated antenna and the EBG-layer.

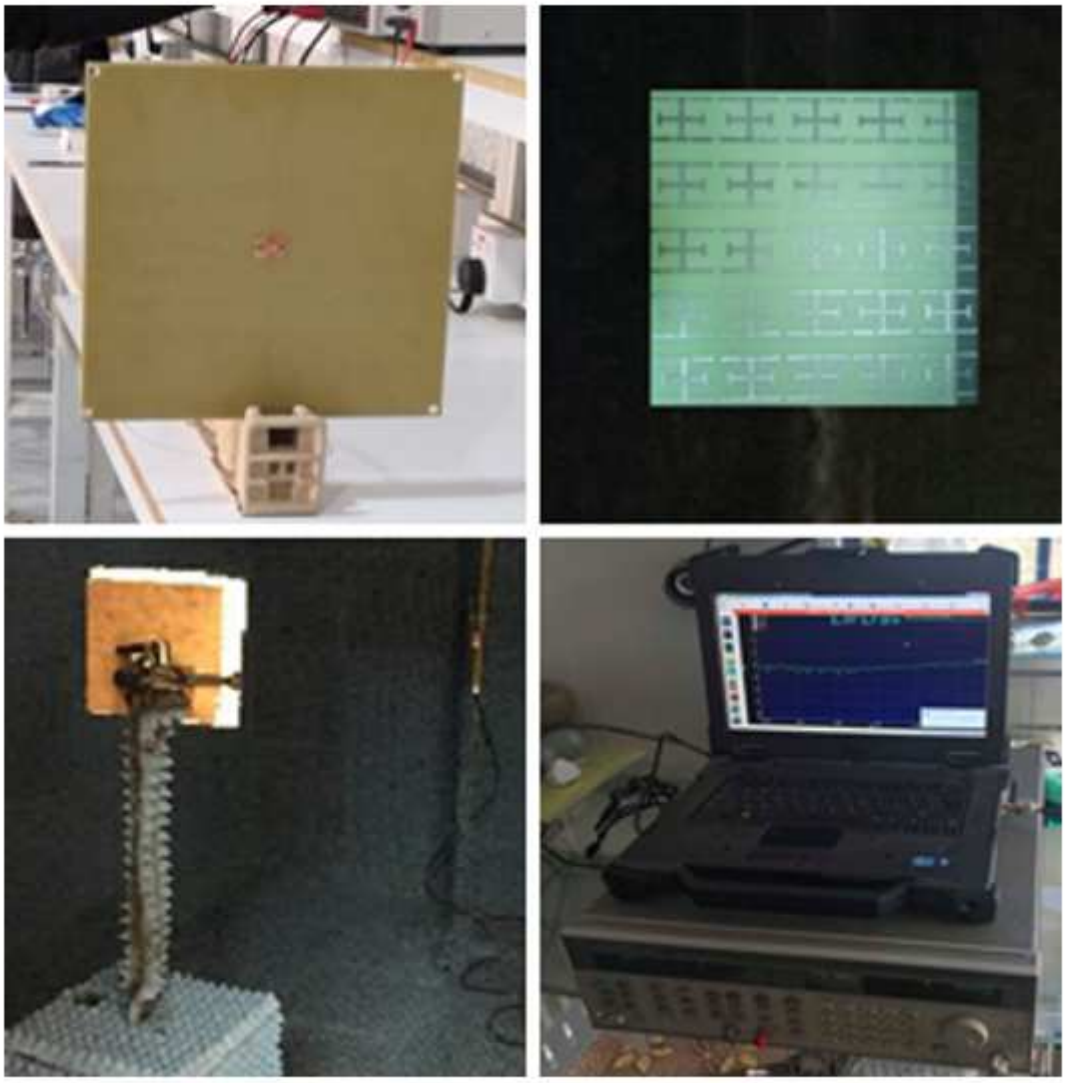

Figure 15

Antenna measurement setup inside the RF anechoic chamber.

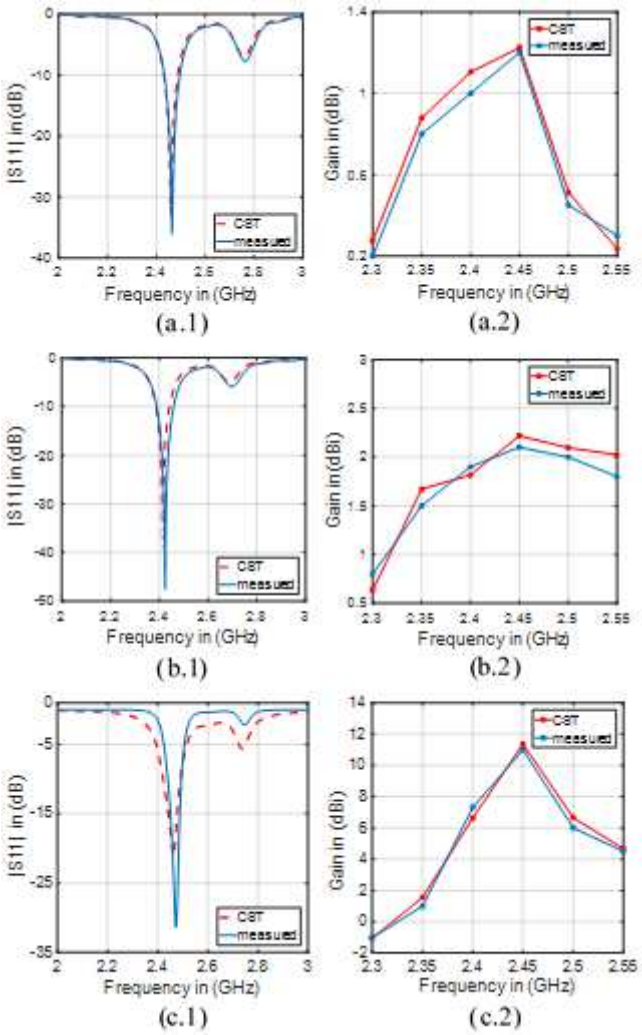

Figure 16

Simulated and measured results for S11 and gain spectra. (a.1) and (a.2) s11 and gain spectra for antenna without EBG layer. (b.1) and (b.2) s11 and gain spectra for antenna with EBG layer based logic_0. (c.1) and (c.2) s11 and gain spectra for antenna with EBG layer based logic_1.

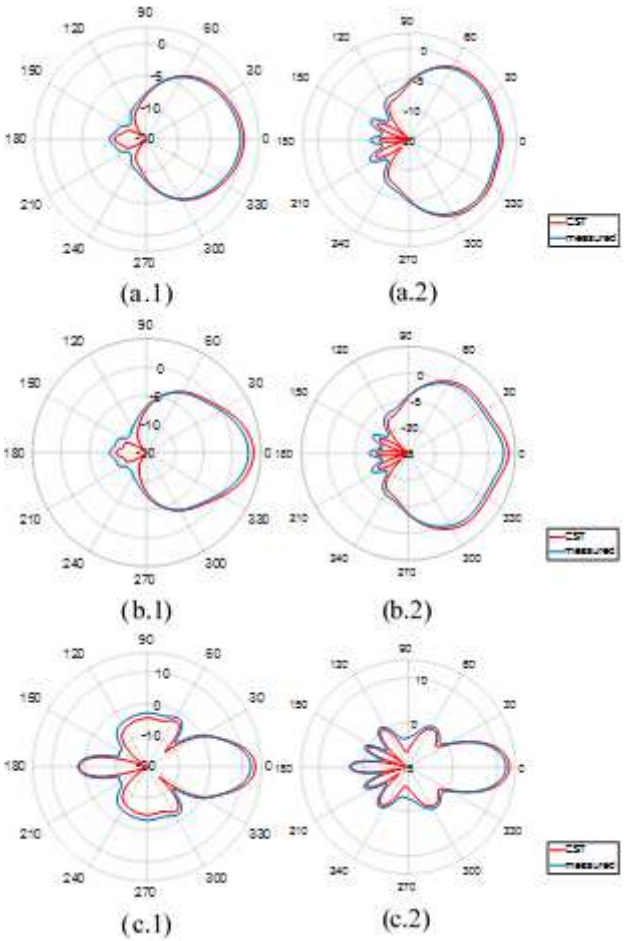

Figure 17

Radiation patterns based simulated and measured results for the proposed antenna: (a.1) and (a.2) without the EBG layer at ϕ=0o and ϕ=90o, respectively. (b.1) and (b.2) with the EBG layer for logic_0 case at ϕ=0o and ϕ=90o, respectively. (c.1) and (c.2) with the EBG layer for logic_1 at ϕ=0o and ϕ=90o, respectively.